Radiation Physics and Chemistry 216 (2024) 111463

Contents lists available at ScienceDirect

Radiation Physics and Chemistry

journal homepage: www.elsevier.com/locate/radphyschem

Evaluation of full-energy-peak efficiencies for a $LaBr_3$:Ce scintillator through a Virtual Point Detector approach

Elio A.G. Tomarchio

Department of Engineering, University of Palermo, Viale Delle Scienze, Building No. 6, I-90128, Palermo, Italy

ARTICLE INFO

Handling Editor: Dr. Chris Chantler

Keywords:
Gamma-ray spectrometry
Virtual point detector
$LaBr_3$:Ce
Counting efficiency

ABSTRACT

The aim of this work is to investigate, in a wide range of gamma-ray energies, the validity of the "Virtual Point Detector" (VPD) approach to evaluate Full-Energy-Peak Efficiency (FEPE) values for a Cerium-doped Lanthanum Bromide scintillator ($LaBr_3$:Ce). With VPD approximation, the detector is assumed equivalent to a virtual point inside the crystal where all the interactions can be considered to occur. The distance of VPD from detector cap is evaluated through experimental point source measurements. The knowledge of the trend of VPD depth as a function of gamma radiation energy allows the evaluation of FEPE values starting from an experimental reference value.

The validation of the procedure has been performed by applying the VPD approach to measurement geometries already characterized such as a disk source, an Havar foil irradiated inside a target of a medical cyclotron, and a parallelepided sample geometry, an atmospheric particulate paper filter reduced to 6 cm × 6 cm × 0.7 cm dimensions. FEPE values determined by VPD approach lead to radionuclide activities very close to the ones already obtained with measurements carried out with other detectors.

1. Introduction

The Cerium-doped Lanthanum Bromide scintillator ($LaBr_3$:Ce) is not yet widespread used with respect to other scintillators although its applications are present in various fields, as nuclear physics (Weisshaar et al., 2008) medical diagnostics (Pani et al., 2006, 2007), nuclear safeguards (Sullivan et al., 2008; Vo, 2008), dosimetry (Camp and Vargas, 2014), and characterization of radioactive waste (Guarino et al., 2007). The improved properties of a $LaBr_3$:Ce scintillator, such as higher energy resolution, faster response time, excellent energy linearity and higher light yield than a common NaI(Tl) scintillator, make it a very interesting tool for various measurement applications. It is noteworthy the possibility of realizing a lightweight portable $LaBr_3$:Ce device for "in situ" gamma-ray spectrometry to be used for environmental monitoring, characterization of contaminated sites or control around nuclear plants (Garnett et al., 2017; Hasan et al., 2022; Ji et al., 2018; Milbrath et al., 2007). However, its use is limited by the intrinsic activity due to the presence of ^{138}La and ^{227}Ac in the detector, with the need for low activity samples to subtract an energy-calibrated background spectrum from the measured one. The use of the scintillator to determine the activity concentration of a radionuclide in a sample requires the knowledge of Full-Energy-Peak Efficiency (FEPE) for the energy of interest or a calibration curve of efficiency as a function of energy. This goal is fullfilled through experimental measurement of a calibrated source with the same shape, composition and density as the sample. Most of the time this source is not available and the efficiencies are determined through a Monte Carlo simulation (Dias et al., 2002; Hasan et al., 2021; Helmer et al., 2003; Vidmar et al., 2008), an analytical approach, if available (Badawi et al., 2012; Boukeffoussa and Bouakaz, 2021; Hamzawy, 2014) or an "efficiency transfer" method (Lepy et al., 2001, 2006; Piton et al., 2000). Each of these methods can be a tedious and time-consuming task that involves the knowledge of detector composition and dimensions.

An interesting opportunity is to extend to $LaBr_3$:Ce detector the concept of Virtual Point Detector (VPD), introduced by Notea (1971) and reported in Debertin and Helmer (1988), to calculate an efficiency value for a measurement geometry starting from a value measured in a reference position. With the VPD approximation, the detector is assumed to be equivalent to a virtual point at which all gamma-ray interactions are considered to occur. Therefore, all physical quantities vary with the square of the distance from the VPD and each efficiency value can be computed from a value measured at a reference point, usually the center of the detector cap. There is no need to know the dimensions and composition of the detector as the evaluation of the VPD distance from the detector cap is carried out by means of experimental

E-mail address: elio.tomarchio@unipa.it.

https://doi.org/10.1016/j.radphyschem.2023.111463
Received 9 September 2023; Received in revised form 16 November 2023; Accepted 7 December 2023
Available online 12 December 2023

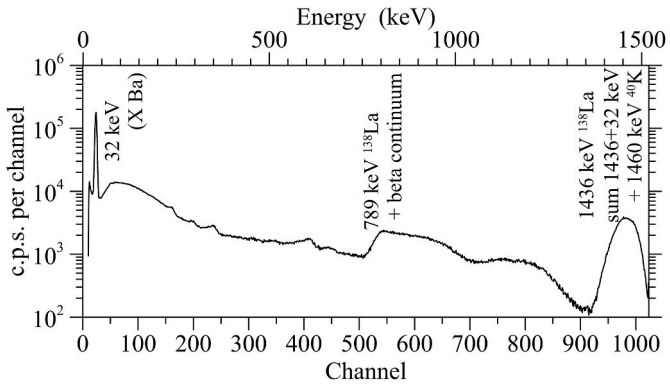

Fig. 1. Gamma-ray spectrum of the background of a bare $LaBr_3$:Ce detector.

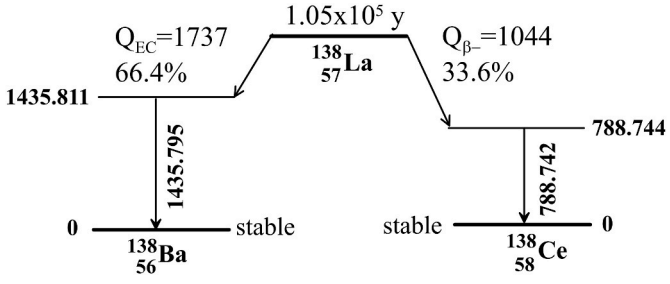

Fig. 2. ^{138}La decay scheme. Energy data in keV.

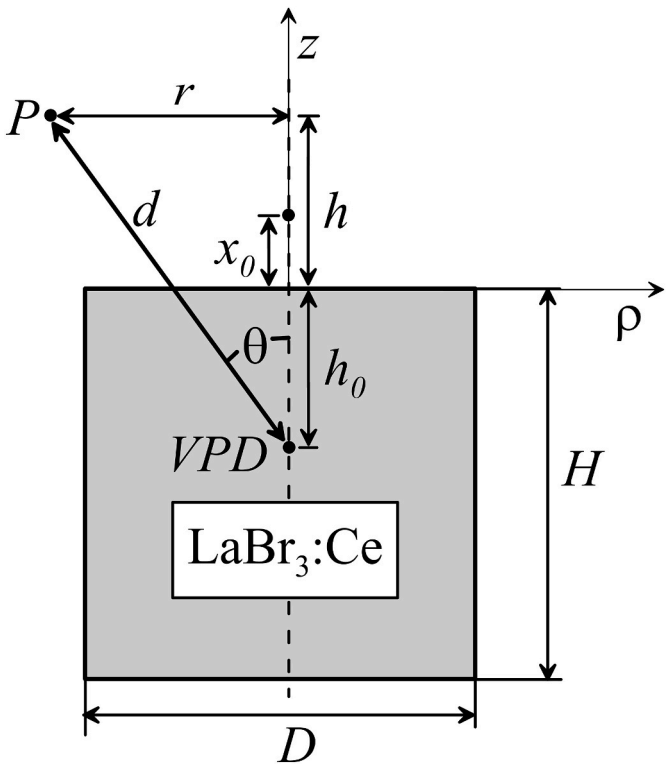

Fig. 3. Schematic representation of the measurement geometry for a point source with VPD approximation.

measurements of point sources.

The VPD concept was extensively applied to Si(Li) detector (Alfassi and Othman, 1977), HPGe detectors (Alfassi et al., 2006, 2007; Hoover, 2007; Mahling et al., 2006; Mohammadi et al., 2011; Presler et al., 2002, 2004; Rizzo and Tomarchio, 2010), NaI(Tl) and BGO scintillators (Presler et al., 2006). Its validity has been demonstrated also for sources located off-axis of the detector (Presler et al., 2002) as well as for volume sources (Presler et al., 2004), while the dependence of the VPD position on the detector size has been highlighted for HPGe detectors in (Mahling et al., 2006) and for scintillators in (Chuong et al., 2020; Rubin et al., 2019).

The aim of this work is to study the validity of the VPD simplification to evaluate the efficiencies of a $LaBr_3$:Ce, a detector not directly considered in the above cited papers. The experimental validation has been carried out referring to a disk-shaped source, an Havar foil activated inside a target of a medical cyclotron and substituted during periodic maintenance, and a parallelepiped source, a paper filter used for the sampling of atmospheric particulate and reduced to a "packet-sample" with dimensions 6 cm × 6 cm × 0.7 cm. Both samples were already characterized and radionuclide activities were previously determined using other methods and detectors (Cannizzaro et al., 1994; Tomarchio, 2013, 2014).

2. Materials and methods

2.1. The $LaBr_3$:Ce detector

A $LaBr_3$:Ce crystal, supplied by Saint-Gobain™, type BrilLanCe-380, size ∅2″×2″, directly coupled to a PMT Photonis XP5500 photomultiplier is used for this investigation (Saint-Gobain Crystals, 2009). The scintillator, the photomultiplier and the magnetic screen are sealed in an aluminum container to avoid hygroscopicity.

The detector is coupled to an ORTEC portable multichannel with USB-Multichannel interface (1024 channels) mod. Digibase™. The acquisition and analysis of spectrometric data is performed using the EG&G ORTEC Maestro analysis software for Windows™, version 7.0 (ORTEC, 2012). The uncertainties associated with the photopeak areas are computed using the peak analysis routine of the ORTEC software. The same range of channels (ROI, Region of interest) has been adopted in all the measurements to avoid errors related to ROI variations.

The characteristics of this type of detectors have been extensively studied in (Alzimami et al., 2008; Iltis et al., 2006; Quarati et al., 2007; Van Loef et al., 2002]. Fig. 1 reports a typical background gamma-ray spectrum where the main features of the detector intrinsic background can be recognized. In fact, with reference to the decay scheme of Fig. 2, a significant peak around 32 keV (related to X emissions of Ba) and a large multiplet between 1430 and 1470 keV (due to the photon emission at 1436 keV of ^{138}La and to the coincidence of the same emission with X of Barium at 32 keV), are easily identified. In the last multiplet the contribution of the 1460 keV emission of ^{40}K, present in most environmental sample measurements, can be considered included and unresolved with respect to other components. This somewhat impairs the use of the instrument for measuring sample with potassium compounds. Furthermore, the spectrum is characterized by a wide distribution due to the continuous beta and the gamma emission of 789 keV (β^- decay) which increases the detection limit in the referred energy range. Background peaks to be attributed to ^{227}Ac (half-life = 21.7 years) are not highlighted in the spectrum of Fig. 1 because they fall within the 1800–3000 keV energy range (Saint-Gobain Crystals, 2009).

Despite this, its high density (5.29 g cm^{-3}), the good energy resolution in the range of energies of interest (about 2.8% at 662 keV of ^{137}Cs), low decay time (26 ns) and high light yield (63 photon per keV), make its use particularly advantageous for the measurement of radioactive samples with few and well-distributed gamma emissions in energy ranges of the spectrum free from background features.

2.2. The VPD approach

With reference to the scheme of Fig. 3, the FEPE value at energy E, $\varepsilon(E,r,h)$, relative to a point source placed at the coordinate position r and

h, can be computed using the VPD method with the simple relationship (Presler et al., 2002)

$$\varepsilon(E,r,h)=\varepsilon(E,0,0)\frac{h_0(E)^2}{r^2+[h+h_0(E)]^2} \quad (1)$$

where, $\varepsilon(E,0,0)$ is FEPE value measured at the center of detector cap and h_0(E) is the distance of the VPD from the detector cap for gamma radiation energy, E. To determine $h_0(E)$ values, a series of spectrometric measurements of gamma radiations of different energy emitted by "single line" sources, i.e. that emit a single gamma line, has been carried out. For each energy E, assumed the center of the detector as the origin of the reference system (see Fig. 3), the value $h_0(E)$ is the inverse of the slope of a linear fit to the experimental values of

$$R(E,0,h)-1=\sqrt{\frac{C(E,0,0)}{C(E,0,h)}}-1=\frac{h}{h_0(E)} \quad (2)$$

where $C(E,0,0)$ and $C(E,0,h)$ are the count rates under the photopeak corresponding to the energy E at the reference position ($r=0$; $h=0$) and at the coordinate point ($r=0$, h), respectively (Alfassi et al., 2006, 2007).

The experimental count rates have been obtained by measuring "single-line" point sources of ^{241}Am, ^{109}Cd, ^{57}Co, ^{137}Cs, ^{54}Mn, ^{65}Zn supplied by CEA and Eckert&Ziegler (activity uncertainties: 1.5–3%; for ^{109}Cd 5%). Point single-line sources of ^{198}Au (gamma emission at 411 keV, half-life = 2.69 days) and ^{203}Hg (gamma emission at 279 keV, half-life = 46.6 days), produced by neutron activation in a neutron irradiator with 4 Am–Be sources, each with 111 GBq activity, have been added (Buffa et al., 2013). The precision and accuracy in determining the activity of the latter sources is not of concern since the evaluation of $h_0(E)$ is carried out by calculating the count rate ratios.

In all measurements performed on axis of the detector, the counting time was enough to ensure good statistical uncertainties (<1%; peak area $>10^4$ counts). The use of single-line sources avoids coincidence-summing corrections for measurements carried out at low distances from the detector, while source activities are such as to reduce the dead time and the pile-up correction to not significant values.

For sources with low half-life a correction for decay during a counting period is needed and has been performed with the simple relationship (Nir-El, 2013)

$$C(t_0)=C(t)\frac{\lambda e^{\lambda T_w}}{(1-e^{-\lambda T_c})} \quad (3)$$

where T_W, T_C are respectively the decay time and the real count time, λ the decay constant and $C(t_0)$ is the correct count rate at a reference date (t_0).

The use of "non single-line" sources is not recommended due to coincidence-summing effects at close distances from the detector cap. However, coincidence-summing correction factors can be calculated through a Monte Carlo simulation, as suggested in (Chuong et al., 2020), or using suitable relations as the ones reported in (Tomarchio and Rizzo, 2011) still considered valid for $LaBr_3$:Ce scintillator. The last procedure is more complex due to difficulties on determination of total efficiency and FEPE for each distance from the detector cap. The main source of error concerns the total efficiency calculation for which is needed a "zero-energy" extrapolation both for the source and background spectrum. Differentiating contribution of the background spectrum as the one presented in Fig. 1 from the one related only to the source is a complex task the result of which may not be reliable.

More interesting is to take into account measurements performed at a distance from the detector cap more than a reference one, x_0, with the hypothesis that at x_0 coincidence-summing effects can be considered statistically negligible. Following these assessments, sources of ^{60}Co, ^{133}Ba and ^{152}Eu, supplied by Amersham (activity uncertainty: 3%) have been also used. For the latter sources, relation (2) was modified with C

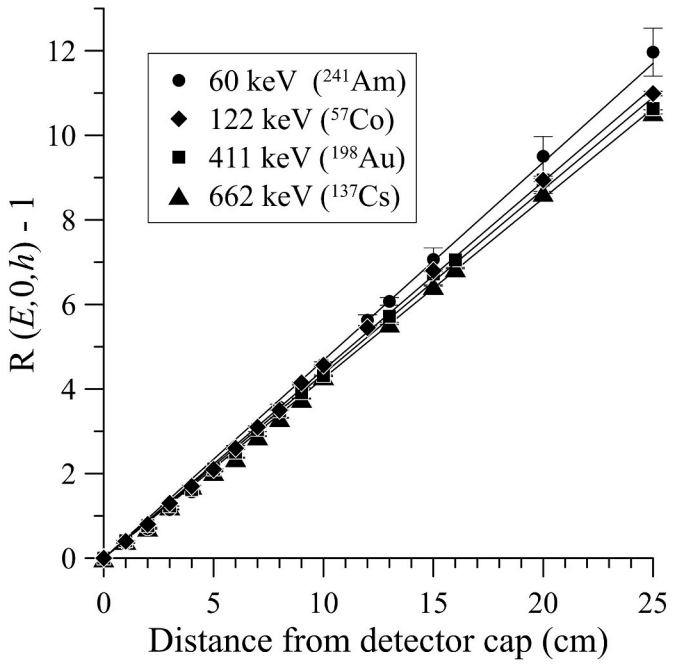

Fig. 4. Linear interpolation to the experimental values of $R(E,0,h)-1$ as a function of the distance from the detector cap. Uncertainties are quoted for a coverage factor k = 1.

$(E,0,x_0)$ the count rate at the reference distance while C$(E,0,h)$ is the one at a distance $h > x_0$ on detector axis. However, the choice of the reference distance x_0 must be done carefully because increasingly low count rates with distance may involve significant increase in statistical uncertainties.

The same VPD approach can be used for a volume source, considering the absorbing matrix as constituted by a quite large number of elementary volumes (assumed as point sources) whose gamma emissions are attenuated in the path length traveled by the photons in the sample. The attenuation coefficient is variable with energy E and related to the composition of the matrix (Presler et al., 2004). Assuming as reference position the center of the detector cap, relation (1) is therefore changed to

$$\varepsilon(E,r,h)=\varepsilon(E,0,0)\frac{h_0(E)^2}{r^2+[h+h_0(E)]^2}\,e^{-\mu(E)\,d_s} \quad (4)$$

where $\mu(E)$ is the linear attenuation coefficient for the sample material at gamma energy, E, and d_s is the path length traveled by the photon in the sample. The determination of d_s for various volume samples and measurement geometries can be obtained through formulations reported in literature as a function of angle θ (Fig. 3) with more or less complex relationships with reference to the measurement geometry, e.g. in (Abbas et al., 2020; Badawi et al., 2014). In the case of volume samples placed on the detector cap and in axis with the scintillator, equation (4) can be specified in

$$\varepsilon(E,r,h)\;=\;\varepsilon(E,0,0)\,\frac{h_0(E)^2}{r^2+[h+h_0(E)]^2}\,e^{-\mu(E)\left(\frac{h}{h+h_0(E)}\sqrt{r^2+[h+h_0(E)]^2}\right)} \quad (5)$$

and the trend of the coefficient $\mu(E)$ can be obtained with reference to data reported in most used manuals, e.g. in (Hubbell and Seltzer, 1996). Otherwise, when specific data for the matrix under examination are not available, an experimental determination of $\mu(E)$ can be carried out by setting single-line reference sources in a collimator around the detector. In this way, from the measurement of the source without any

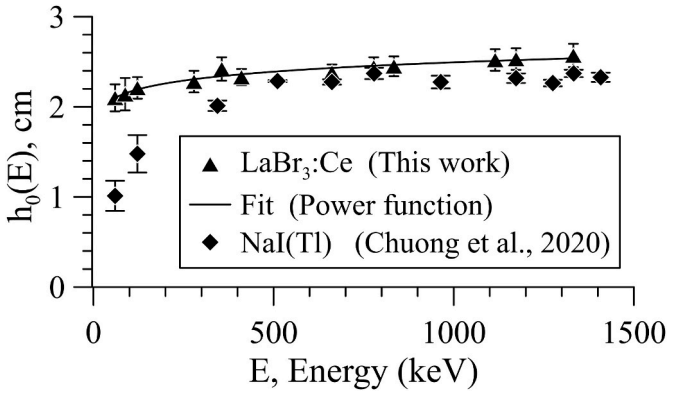

Fig. 5. Trend of h_0 values as a function of energy compared with the ones relative to a NaI(Tl) scintillator with the same dimensions. Uncertainties are quoted for a coverage factor k = 1. Data are fitted with a power function (R^2 = 0.956, p < 0.0001).

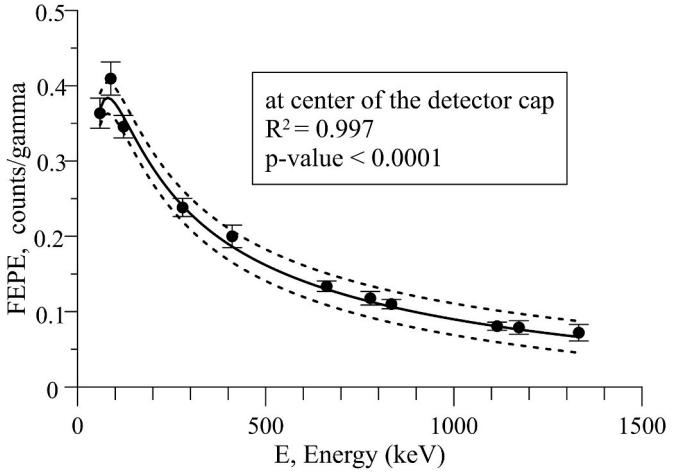

Fig. 6. FEPE trend for point sources located at the center of the cap of the LaBr$_3$:Ce detector. Uncertainties are quoted for a coverage factor k = 1. Solid line represents the best fit to experimental data, dotted lines highlight 95% confidence interval around the fit.

attenuation (I_0) and the one with interposed the matrix of interest (I), the value of the attenuation coefficient for a given energy E is obtained through the simple relationship

$$\mu(E) = \frac{\ln\left(\frac{I_0(E)}{I(E)}\right)}{x} \quad (6)$$

where x is the thickness of the sample.

3. Results and discussion

3.1. The $h_0(E)$ curve

Fig. 4 shows the trend of the ratio (2) for some gamma emissions originating from single-line sources. Trends for other energies are not reported for clarity of representation. It should be noted that the correlation coefficients for each linear interpolation are quite high (R^2 ranges between 0.988 and 0.999). The inverse of the slope of the linear fit represents the value of $h_0(E)$. An analogous trend occurs for non single-line sources with measurements carried out with distances more than a value x_0 equal to 10 cm.

The $h_0(E)$ behaviour as a function of energy is shown in Fig. 5. The experimental data are well fitted with a power function (correlation index R^2 = 0.956, p-value <0.0001). The same Fig. 5 shows also the values of $h_0(E)$ reported in (Chuong et al., 2020) for a NaI(Tl) scintillator with the same dimensions of the LaBr$_3$:Ce detector. It can be seen that the values differ significantly in the low energy range, due to different densities and efficiencies of the detectors, while the difference is reduced in the high energy range. However the $h_0(E)$ values for LaBr$_3$:Ce detector are always larger than the ones of a similar NaI(Tl) detector with an almost flat variation trend with energy.

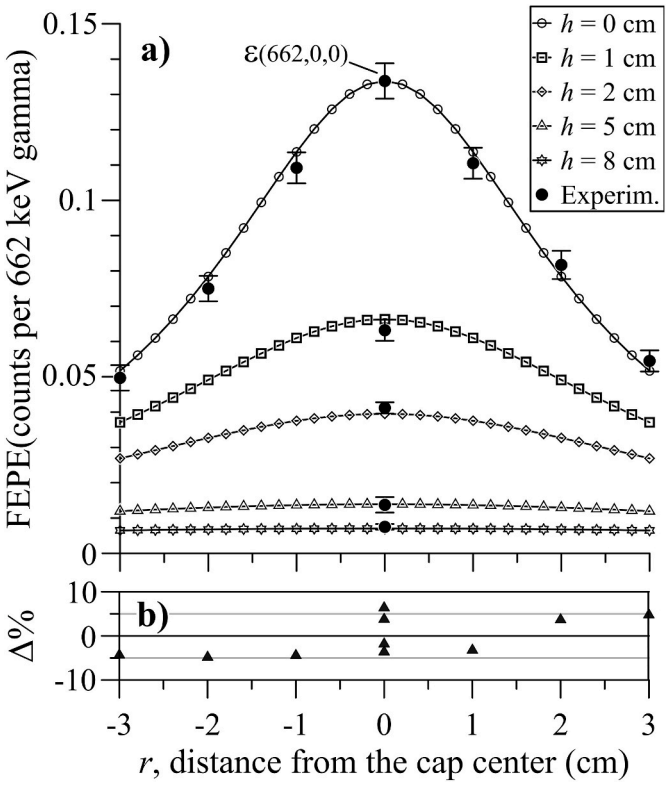

Fig. 7. (a) Trend of VPD point source FEPE values vs radius for 662 keV energy of ^{137}Cs at various positions around the detector compared with experimental values (filled symbol). Uncertainties are quoted for a coverage factor k = 2. (b) Percentage differences computed as $\Delta\% = 100\cdot(\varepsilon_{exp}(662,r,h) - \varepsilon_{VPD}(662,r,h))/\varepsilon_{exp}(662,r,h)$.

3.2. Efficiency evaluation

The knowledge of $h_0(E)$ behaviour allows to determine the efficiencies for a point source in the position of coordinates (r,h) through relation (1). For volume source with a given absorbing matrix, the use of relation (4) allows to obtain the elementary efficiency for a portion of source to be integrated over its whole volume. The only necessary data are efficiency values in a reference position, for example the values at the center of the scintillator cap, $\varepsilon(E,0,0)$, normally available for any detector. Fig. 6 reports for the LaBr$_3$:Ce detector the experimental efficiencies at center of the cap, $\varepsilon(E,0,0)$, in the energy range 60–1332 keV, fitted with a 4th degree polynomial curve referred to logarithmic values. The goodness of fit is verified by a correlation index R^2 = 0.997, a p-value less than 0.0001 and highlighting a 95% confidence interval around the fit computed following the method reported in (Brown, 2001).

As an example of the method application, Fig. 7 a) report the trends of VPD evaluated point source efficiency values for 662 keV emission of ^{137}Cs (empty symbols) with reference to a system whose origin is the center of the detector cap. For comparison, the values of experimental FEPE measured with a ^{137}Cs point source at various distances both along the axis of the detector and in the radial direction are also reported

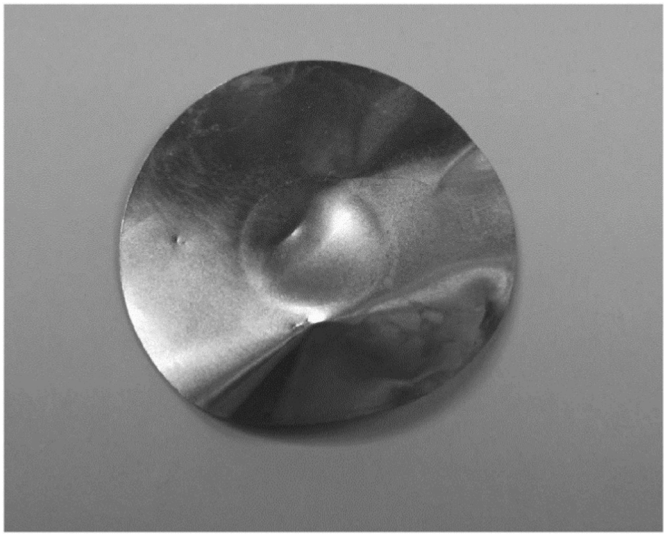

Fig. 8. Photograph of an Havar® foil replaced during maintenance after an irradiation cycle.

(filled symbols). The percentage differences showed in Fig. 7 b) demonstrate the goodness of h_0(662 keV) evaluation as values are almost all less than 5%.

3.3. Experimental validation

As a validation, the procedure has been applied for the analysis of an Havar foil (30 mm in diameter, 50 μm thick) of a IBA CYCLONE 18/9 target irradiated at the Nuclear Medicine Center "S. Gaetano" in Bagheria (a town near Palermo, Italy) and replaced during a maintenance. Fig. 8 reports a photograph of the Havar foil.

The verify is performed by comparison of radionuclide activity determinations through VPD approach with the ones obtained in (Tomarchio, 2014). Assuming an uniform activity distribution on disk source of radius R, placed on the cap of the detector, disk source efficiency $\varepsilon_{disk}(E)$ can be computed using the relation (Radu et al., 2009)

$$\varepsilon_{disk}(E,R) = \frac{2\pi \int_0^R \varepsilon_r(E,r)\, r dr}{\pi R^2} \tag{7}$$

where $\varepsilon_r(E,r)$ is the VPD efficiency of a point (elementary) source placed on the detector cap ($h = 0$) at distance r from the detector axis. As the thickness of foil is very small, does not take into account any absorption correction. The measurement geometry is shown in Fig. 9 a). For the evaluation of the disk efficiency at the various energies, reference values $\varepsilon(E,0,0)$ have been derived from curve shown in Fig. 6. The value of elementary efficiency $\varepsilon(E,r)$, representative of an annulus with a mean radius r and a 0.1 mm thickness (difference between outer and inner radius) can be obtained through eqn. (1). Following eq. (7), the value of the disk efficiency at a given energy is obtained summing all the contributions normalized over the whole disk area.

The gamma-ray spectrum of Fig. 9 b) detected on the Havar foil after 4400 days decay time allows to highlight peaks of ^{57}Co, ^{54}Mn and ^{60}Co and to evaluate activities to compare with the data reported in (Tomarchio, 2014). For 122 keV emission of ^{57}Co, an efficiency value equal to 0.28 ± 0.04 counts/gamma and an activity of 192 ± 13 Bq is computed and, taking into account the decay time, an extraction activity value of (2.01 ± 0.13) × 10^4 kBq is derived. This value is to be compared with the value reported in (Tomarchio, 2014) of (1.91 ± 0.05) × 10^4 kBq, with a percentage difference of 5.2% that is not significant in relation to data uncertainties.

For 834 keV emission of ^{54}Mn an efficiency of 0.091 ± 0.008 counts/gamma and an activity value of 101 ± 10 Bq is calculated, which, considering the decay time, leads to a value of 2480 ± 250 Bq against the 2420 ± 80 Bq value reported in (Tomarchio, 2014). In this case the percentage difference of about 3% is well below the statistical uncertainties of the measurements.

For ^{60}Co, computed the efficiency values of 0.06 ± 0.01 and 0.05 ± 0.01 counts/gamma for gamma emission at energies 1173 and 1332 keV, respectively, a mean activity value of 656 ± 86 Bq was obtained. At extraction time, calculated activity of 3.44 ± 0.45 kBq is compared to 3.6 ± 0.1 kBq value reported in (Tomarchio, 2014), with a percentage difference of about 5%.

The same VPD approach has been adopted for a volume source consisting of a cellulose filter used for the filtration of atmospheric air particulate and reduced, at the end of the suction, to strips which are then stacked and pressed by a means of a 15-tons press to obtain a volume of 6 cm × 6 cm × 0.7 cm. The final density is approximately 0.8 g cm^{-3}. Fig. 10 report photographs of a filter at the end of suction and

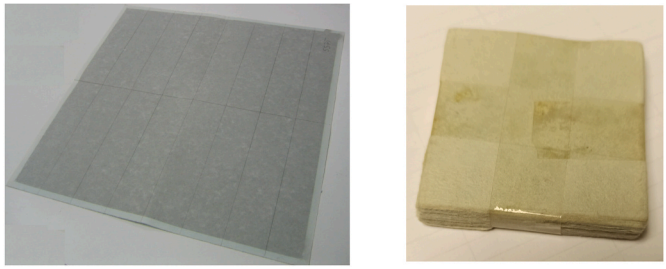

Fig. 10. Photographs of Sofiltra-Poelman HYN-75 45 cm × 45 cm cellulose filter paper at the end of air particulate collection and reduced to a 6 cm × 6 cm × 0.7 cm packet-sample [Cannizzaro et al., 1994].

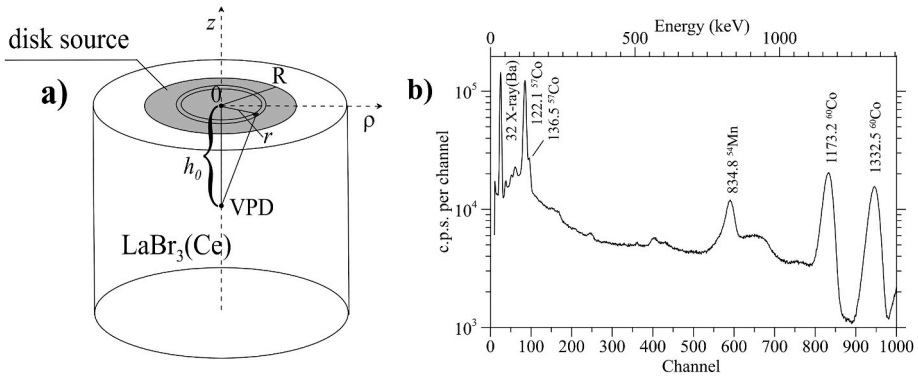

Fig. 9. (a) Schematic design of Havar disk measurement geometry. (b) Gamma-ray spectrum detected with $LaBr_3$:Ce on Havar foil after 4400 days decay (b).

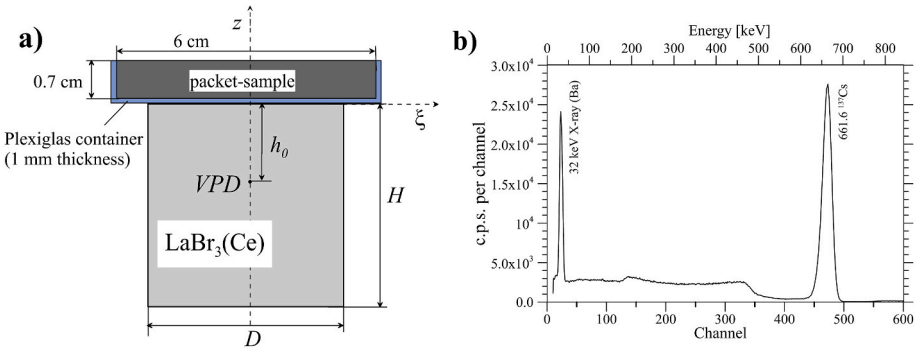

Fig. 11. (a) Sketch of the measurement geometry for the air particulate filter (reduced to a packet sample) on the top of $LaBr_3$:Ce detector. (b) Gamma-ray spectrum of filter No. 944 taken on May 01, 1986, and measured on September 30, 2019 (decay: 12,205 days) which highlights the presence of only 662 keV peak (^{137}Cs).

Table 1
Uncertainty budget.

Geometry	Source of uncertainty	Magnitude	Notes
Point source	Photopeak area	<1 %	Eqn. (1)
	Source activity	<3%	Manufacturer data
	Emission probability	<1.5 %	Literature data
	Live time, Source position	Negligible	MCA option Eqn. (2), Data fit
	h_0(E)	<2 %	Eqn.(1), Eqn.(3)
	Decay correction	<0.1 %	Single-γ emitter
	Coincidence-summing	Negligible	source
	Pile-up correction	Negligible	
	Combined uncertainty	<4 %	
Volume source	attenuation coefficient	<3%	Eqn. (4)
	Combined uncertainty	<5 %	

reduced to a "packet-sample" dimensions useful to perform spectrometric measurements. It can be considered constituted by a quite large number of elementary volumes (considered as point sources) whose gamma emissions are attenuated in the path length traveled by the photon in the sample with an attenuation coefficient related to gamma energy and the composition of the matrix. The overall efficiency is determined by integration of elementary efficiencies over the whole volume through the relationship (5). The measurement geometry is represented in Fig. 11 where the thickness of 1 mm Plexiglas of the filter container used for the measurement is also highlighted. The attenuation coefficient μ(662) is determined experimentally by measuring a source of ^{137}Cs in a collimated system, without and with a variable number of packet-sample interposed. From respective count rate values, a coefficient μ(662 keV) = 0.051 cm^{-1} is evaluated through the relation (6). Similarly, an attenuation coefficient of μ(662 keV) = 0.1 cm^{-1} has been experimentally determined by interposing a thickness of Plexiglas. The last result is very close to the value of 0.107 cm^{-1} calculated from data reported in (Hubbell and Seltzer, 1996) for polymethyl methacrylate (Plexiglas) composite material.

Taking into consideration only a quarter of the sample, due to symmetry of the geometry, the values of elementary efficiencies for 252 vol of 0.5 cm × 0.5 cm × 0.1 cm dimensions are computed. Then, integrating over the whole volume of the sample the contribution of each volume element, a value of 0.057 counts/gamma of 662 keV is obtained, including the attenuation of the interposed Plexiglas thickness. There are no significant variation if the number of volume elements are increased (e.g. with volumes of dimensions 0.2 cm × 0.2 cm × 0.1 cm the difference is not greater than 1%). This value is then compared with the experimental efficiency value of 0.055 counts/gamma of 662 keV, obtained from the measurement of the particulate sample collected in the period of maximum concentration following the Chernobyl accident, whose ^{137}Cs activity was well characterized in previous analyses (Cannizzaro et al., 1994). The gamma-ray spectrum detected on the last measurement on the sample is showed in Fig. 11 b).

The difference between the two values of about 3.6 % is not significant in relation to the uncertainties related to measurement data, activities of the source and attenuation coefficients.

Indeed, with reference to equations (1)–(4), the uncertainty budget is mainly related to errors on evaluating reference efficiencies, ε(E,0,0), to determination of $h_0(E)$ values, and, for volume sources, to the attenuation coefficients.

Table 1 reports the evaluation of the uncertainty budget, set following directions reported in (Ceccatelli et al., 2017) and taking into account the variability of data for each radionuclide. Finally, the combined uncertainties to be associated to FEPE values can be considered acceptable as estimated less than 5 %.

4. Conclusions

The technique of assimilating the detector to a virtual point allows to determine the efficiencies for a $LaBr_3$:Ce scintillator for a given measurement geometry quite simply and quickly with biases less than 5 % with respect to experimental values. After determining the trend of variation of the depth of the VPD in the crystal as a function of energy, the only necessary data are the FEPE values in a reference point, usually available for each of gamma radiation detectors. The values of the efficiencies in various points around the detector can be then calculated with a simple spreadsheet, avoiding more complex procedures or Monte Carlo simulation.

The aim of this work is fulfilled since the VPD approach is verified to be applicable to $LaBr_3$:Ce detector and the corresponding efficiencies, even with volume samples, does not differ significantly from the corresponding experimental values. Therefore, VPD simplified approach represents a reliable tool for $LaBr_3$:Ce scintillator efficiencies evaluating and radionuclide activity determining in samples of various shape.

Declaration of competing interest

The author declares that he has no known competing financial interests or personal relationships that could have appeared to influence the work reported in this paper.

Data availability

Data will be made available on request.

Acknowledgements

This work is supported by F.F.R. (Fondo Finanziamento Ricerca) funds of University of Palermo, years 2018–2021. The $LaBr_3$:Ce scintillator and electronic instrumentation were acquired with European funds included in the POR Sicilia 2000–2006 plan.

References

Abbas, M.I., Badawi, M.S., Thabet, A.A., et al., 2020. Efficiency of a cubic NaI(Tl) detector with rectangular cavity using standard radioactive point sources placed at non-axial position. Appl. Radiat. Isot. 163, 109139 https://doi.org/10.1016/j.apradiso.2020.109139.

Alfassi, Z.B., Othman, R., 1977. Off-center X-ray detection efficiencies of Si(Li) detectors. Nucl. Instrum. Methods 143, 57. https://doi.org/10.1016/0029-554X(77)90330-5.

Alfassi, Z.B., Pelled, O., German, U., 2006. The virtual point detector concept for HPGe planar and semi-planar detectors. Appl. Radiat. Isot. 64, 574. https://doi.org/10.1016/j.apradiso.2005.11.007.

Alfassi, Z.B., Lavi, N., Presler, O., Pushkarski, V., 2007. HPGe virtual point detector for radioactive disk sources. Appl. Radiat. Isot. 65, 253. https://doi.org/10.1016/j.apradiso.2006.08.002.

Alzimami, K., Abuelhia, E., Podolyak, Z., Ioannou, A., Spyrou, N.M., 2008. Characterization of $LaBr_3$:Ce and $LaCl_3$:Ce scintillators for gamma-ray spectroscopy. J. Radioanal. Nucl. Chem. 278 (3), 755. https://doi.org/10.1007/s10967-008-1606-6.

Badawi, M.S., Gouda, M.M., Nafee, S.S., et al., 2012. New analytical approach to calibrate the co-axial HPGe detectors including correction for source matrix self-attenuation. Appl. Radiat. Isot. 70 (12), 2661. https://doi.org/10.1016/j.apradiso.2012.08.014.

Badawi, M.S., Ruskov, I., Gouda, M.M., et al., 2014. A numerical approach to calculate the full-energy-peak efficiency of HPGe well-type detectors using the effective solid angle ratio. J. Instrum. 9 (7), P07030 https://doi.org/10.1088/1748-0221/9/07/P07030.

Boukeffoussa, K., Bouakaz, K., 2021. Analytical method for calculating the efficiency and solid angle of an NaI(Tl) detector. Appl. Radiat. Isot. 173, 109708 https://doi.org/10.1016/j.apradiso.2021.109708.

Brown, A.M., 2001. A step-by-step guide to non-linear regression analysis of experimental data using a Microsoft Excel spreadsheet. Comput. Methods Progr. Biomed. 65 (3), 191. https://doi.org/10.1016/S0169-2607(00)00124-3.

Buffa, P., Rizzo, S., Tomarchio, E., 2013. A Monte Carlo-aided design of a modular ^{241}Am-Be neutron irradiator. Nucl. Technol. Radiat. Protect. XXVIII (3), 265, 10.22989NTRP/1303265B.

Camp, A., Vargas, A., 2014. Ambient dose estimation H*(10) from $LaBr_3$(Ce) spectra. Radiat. Protect. Dosim. 160 (4), 264. https://doi.org/10.1093/rpd/nct342.

Cannizzaro, F., Greco, G., Raneli, M., Spitale, M.C., Tomarchio, E., 1994. Determination of radionuclide concentrations in the air of Palermo from the Chernobyl accident to December 1992. Nucl. Geophys. 8 (4), 373 (available from: author upon request).

Ceccatelli, A., Dybdal, A., Fajgelj, A., Pitois, A., 2017. Calculation spreadsheet for uncertainty estimation of measurement results in gamma-ray spectrometry and its validation for quality assurance purpose. Appl. Radiat. Isot. 124, 7–15. https://doi.org/10.1016/j.apradiso.2017.03.002.

Chuong, H.D., Trang, L.N., Nguyen, V.H., Thanh, T.T., 2020. A revision of the virtual point detector model for calculating NaI(Tl) detector efficiency. Appl. Radiat. Isot. 162, 109179 https://doi.org/10.1016/j.apradiso.2020.109179.

Debertin, K., Helmer, R.G., 1988. Gamma- and X-Ray Spectrometry with Semiconductor Detectors. North-Holland, Amsterdam, New York, pp. 250–252.

Dias, M.S., Takeda, M.N., Koskinas, M.F., 2002. Cascade summing corrections for HPGe spectrometers by the Monte Carlo methods. Appl. Radiat. Isot. 56, 105. https://doi.org/10.1016/s0969-8043(01)00174-9.

Garnett, R., Prestwich, W.V., Atanackovic, J.M., Wong, M., Byun, S.H., 2017. Characterization of a $LaBr_3$(Ce) detector for gamma-ray spectrometry for CANDU power reactors. Radiat. Meas. 106, 628. https://doi.org/10.1016/j.radmeas.2017.03.042.

Guarino, P., Rizzo, S., Tomarchio, E., Greco G., 2007. Gamma-ray spectrometric characterization of waste activated target components in a PET Cyclotron, CYCLOTRON 2007 - *18th International Conference on Cyclotron and their Application*, Giardini Naxos (ME), 30 September- 5 October 2007. Available at http://accelconf.web.cern.ch/AccelConf/c07/PAPERS/295.pdf.

Hamzawy, A., 2014. New analytical approach to calculate the detector efficiencies of NaI (Tl) using coaxial and off-axis rectangular and parallelepiped sources. Nucl. Instrum. Methods A768, 164. https://doi.org/10.1016/j.nima.2014.09.013.

Hasan, M., Vidmar, T., Rutten, J., Verheyen, L., Camps, J., Huysmans, M., 2021. Optimization and validation of a $LaBr_3$(Ce) detector model for use in Monte Carlo simulations. Appl. Radiat. Isot. 174, 109790 https://doi.org/10.1016/j.apradiso.2021.109790.

Hasan, M.M., Rutten, J., Camps, J., Huysmans, M., 2022. Minimum detectable activity concentration of radio-cesium by a $LaBr_3$(Ce) detector for in situ measurements on the ground-surface and in boreholes. Appl. Radiat. Isot. 185, 110247 https://doi.org/10.1016/j.apradiso.2022.110247.

Helmer, R.G., Hardy, J.C., Iacob, V.E., Sanchez-Vega, M., Neilson, R.G., Nelson, J., 2003. The use of Monte Carlo calculations in the determination of a Ge detector efficiency curve. Nucl. Instrum. Methods A511, 360. https://doi.org/10.1016/S0168-9002(03)01942-9.

Hoover, A., 2007. Characterization of the virtual point detector effect for coaxial HPGe detectors using Monte Carlo simulation. Nucl. Instrum. Methods 572, 839. https://doi.org/10.1016/j.nima.2006.12.031.

Hubbell, J.H., Seltzer, S.M., 1996. X-ray mass attenuation coefficients. NIST Standard Reference Database 126. https://www.nist.gov/pml/x-ray-mass-attenuation-coefficients.

Iltis, A., Mayhugh, M.R., Menge, P., Rozsa, C.M., Selles, O., Solovyev, V., 2006. Lanthanum halide scintillators: properties and applications. Nucl. Instrum. Methods A 563, 359. https://doi.org/10.1016/j.nima.2006.02.192.

Ji, Y.-Y., Choi, H.-Y., Lee, W., Kim, C.-J., Chang, H.-S., Chung, K.-H., 2018. Application of a $LaBr_3$(Ce) scintillation detector to an environmental radiation monitor. IEEE Trans. Nucl. Sci. 65 (8), 2021. https://doi.org/10.1109/TNS.2018.2823322.

Lepy, M.C., et al., 2001. Intercomparison of efficiency transfer software for gamma-ray spectrometry. Appl. Radiat. Isot. 55 (4), 493. https://doi.org/10.1016/S0969-8043(01)00101-4.

Lepy, M.C., Brun, P., Collin, C., Plagnard, J., 2006. Experimental validation of coincidence summing corrections computed by the ETNA software. Appl. Radiat. Isot. 64, 1340. https://doi.org/10.1016/j.apradiso.2006.02.042.

Mahling, S., Orion, I., Alfassi, Z.B., 2006. The dependence of the virtual point-detector on the HPGe detector dimensions. Nucl. Instrum. Methods A 557, 544. https://doi.org/10.1016/j.nima.2005.11.118.

Milbrath, B.D., Choate, B.J., Fast, J.E., Hensley, W.K., Kouzes, R.T., Schweppe, J.E., 2007. Comparison of $LaBr_3$:Ce and NaI(Tl) scintillators for radioisotope identification devices. Nucl. Instrum. Methods A 572, 774. https://doi.org/10.1016/j.nima.2006.12.003.

Mohammadi, M.A., Abdi, M.R., Kamali, M., Mostajaboddavati, M., Zare, M.R., 2011. Evaluation of HPGe detector efficiency for point sources using virtual point detector model. Appl. Radiat. Isot. 69, 521. https://doi.org/10.1016/j.apradiso.2010.10.024.

Nir-El, Y., 2013. Correction for decay during counting in gamma spectrometry. Radiat. Protect. Dosim. 153 (3), 400. https://doi.org/10.1093/rpd/ncs106.

Notea, A., 1971. The Ge(Li) spectrometer as a point detector. Nucl. Instrum. Methods 91, 513. https://doi.org/10.1016/S0029-554X(71)80031-9.

ORTEC, Maestro-32, 2012. MCA Emulation Software A65-B32, Vers. 7.0, User's Manual, ORTEC. Oak Ridge, TN.

Pani, R., Bennati, P., Betti, M., et al., 2006. Lanthanum scintillation crystals for gamma ray imaging. Nucl. Instrum. Methods A 567, 294. https://doi.org/10.1016/j.nima.2006.05.098.

Pani, R., Pellegrini, R., Cinti, M.N., et al., 2007. $LaBr_3$:Ce crystal: the latest advance for scintillation cameras. Nucl. Instrum. Methods A 572, 268. https://doi.org/10.1016/j.nima.2006.10.364.

Piton, F., Lepy, M.C., Bè, M., Plagnard, J., 2000. Efficiency transfer and coincidence summing corrections for γ-ray spectrometry. Appl. Radiat. Isot. 52, 791. https://doi.org/10.1016/S0969-8043(99)00246-8.

Presler, O., Pelled, O., German, U., Leichter, Y., Alfassi, Z.B., 2002. Off-center efficiency of HPGe detectors. Nucl. Instrum. Methods A484, 444. https://doi.org/10.1016/S0168-9002(01)02056-3.

Presler, O., German, U., Pelled, O., Alfassi, Z.B., 2004. The validity of the virtual point detector concept for absorbing media. Appl. Radiat. Isot. 60, 213. https://doi.org/10.1016/j.apradiso.2003.11.019.

Presler, O., German, U., Pushkarsky, V., Alfassi, Z.B., 2006. Virtual Point detector: on the interpolation and extrapolation of scintillation detectors counting efficiencies. Nucl. Instrum. Methods A565, 704. https://doi.org/10.1016/j.nima.2006.05.261.

Quarati, F., Bos, A.J.J., Brandenburg, S., Dathy, C., Dorenbos, P., et al., 2007. X-ray and gamma-ray response of a 2"×2" $LaBr_3$:Ce scintillation detector. Nucl. Instrum. Methods A 574, 115. https://doi.org/10.1016/j.nima.2007.01.161.

Radu, D., Stanga, D., Sima, O., 2009. A method of efficiency calibration for disk sources in gamma-ray spectrometry. Rom. Rep. Phys. 61 (2), 203. Available at: https://rrp.nipne.ro/2009_61_2/art03Radu.pdf.

Rizzo, S., Tomarchio, E., 2010. Virtual point detector: application to coincidence-summing correction in gamma-ray spectrometry. Appl. Radiat. Isot. 68, 1448. https://doi.org/10.1016/j.apradiso.2009.11.025.

Rubin, T., Brandys, I., Presler, O., 2019. The dependence of the virtual point detector on the scintillation detector dimensions. Nucl. Instrum. Methods A929, 34. https://doi.org/10.1016/j.nima.2019.03.023.

Saint-Gobain Crystals, 2009. BrilLanCe Scintillators Performance Summary, Scintillation Product Technical Note, Rev. January. https://www.gammadata.se/assets/Uploads/SGC-BrilLanCe-Scintillators-Performance-Summary2.pdf.

Sullivan, J.P., Rawool-Sullivan, M.W., Wenz, T.R., 2008. $LaCl_3$(Ce) and $LaBr_3$(Ce) gamma-ray spectra with various plutonium isotopic and uranium enrichment standards. J. Radioanal. Nucl. Chem. 276 (3), 699. https://doi.org/10.1007/s10967-008-0620-z.

Tomarchio, E., 2013. An experimental approach to efficiency calibration for gamma-ray spectrometric analysis of large air particulate filters. Radiat. Phys. Chem. 85, 53. https://doi.org/10.1016/j.radphyschem.2012.11.005.

Tomarchio, E., 2014. Measurement of radionuclide activities induced in target components of an IBA CYCLONE 18/9 by gamma-ray spectrometry with HPGe and $LaBr_3$:Ce detectors. Health Phys. 107 (2), S143. https://doi.org/10.1097/HP.0000000000000128.

Tomarchio, E., Rizzo, S., 2011. Coincidence-summing correction equations in gamma-ray spectrometry with p-type HPGe detectors. Radiat. Phys. Chem. 80, 318. https://doi.org/10.1016/j.radphyschem.2010.09.014.

Van Loef, E.V.D., Dorenbos, P., Van Eijk, C.W.E., Kramer, K.W., Gudel, H.U., 2002. Scintillation properties of $LaBr_3$:Ce^{3+} crystals: fast, efficient and high-energy resolution scintillators. Nucl. Instrum. Methods A 486, 254. https://doi.org/10.1016/S0168-9002(02)00712-X.

Vidmar, T., et al., 2008. An intercomparison of Monte Carlo codes used in gamma-ray spectrometry. Appl. Radiat. Isot. 66, 764. https://doi.org/10.1016/j.apradiso.2008.02.015.

Vo, D.T., 2008. Comparison of portable detectors for uranium enrichment measurements. J. Radioanal. Nucl. Chem. 276 (3), 693. https://doi.org/10.1007/s10967-008-0619-5.

Weisshaar, D., allace, M.S., S, M., Adrich, P., et al., 2008. $LaBr_3$:Ce scintillators for in-beam gamma-ray spectroscopy with fast beams of rare isotopes. Nucl. Instrum. Methods A 594, 56. https://doi.org/10.1016/j.nima.2008.06.008.